REVIEW ARTICLE

Impedance cardiography: Pulsatile blood flow and the biophysical and electrodynamic basis for the stroke volume equations

Donald P. Bernstein

Palomar Medical Center, Escondido, CA, USA
E–mail: strokevolumedon@aol.com

Abstract

Impedance cardiography (ICG) is a branch of bioimpedance primarily concerned with the determination of left ventricular stroke volume (SV). As implemented, using the transthoracic approach, the technique involves applying a current field longitudinally across a segment of thorax by means of a constant magnitude, high frequency, low amplitude alternating current (AC). By Ohm's Law, the voltage difference measured within the current field is proportional to the electrical impedance Z (Ω). Without ventilatory or cardiac activity, Z is known as the transthoracic, static base impedance Z_0. Upon ventricular ejection, a characteristic time dependent cardiac-synchronous pulsatile impedance change is obtained, $\Delta Z(t)$, which, when placed electrically in parallel with Z_0, constitutes the time-variable total transthoracic impedance Z(t). $\Delta Z(t)$ represents a dual-element composite waveform, which comprises both the radially-oriented volumetric expansion of and axially-directed forward blood flow within both great thoracic arteries. In its majority, however, $\Delta Z(t)$ is known to primarily emanate from the ascending aorta. Conceptually, commonly implemented methods assume a volumetric origin for the peak systolic upslope of $\Delta Z(t)$, (i.e. dZ/dt_{max}), with the presumed units of $\Omega \cdot s^{-1}$. A recently introduced method assumes the rapid ejection of forward flowing blood in earliest systole causes significant changes in the velocity-induced blood resistivity variation ($\Delta \rho_b(t)$, $\Omega cm \cdot s^{-1}$), and it is the peak rate of change of the blood resistivity variation $d\rho_b(t)/dt_{max}$ ($\Omega cm \cdot s^{-2}$) that is the origin of dZ/dt_{max}. As a consequence of dZ/dt_{max} peaking in the time domain of peak aortic blood acceleration, dv/dt_{max} ($cm \cdot s^{-2}$), it is suggested that dZ/dt_{max} is an ohmic mean acceleration analog ($\Omega \cdot s^{-2}$) and not a mean flow or velocity surrogate as generally assumed. As conceptualized, the normalized value, $dZ/dt_{max}/Z_0$, is a dimensionless ohmic mean acceleration equivalent (s^{-2}), and more precisely, the electro-dynamic equivalent of peak aortic reduced average blood acceleration (PARABA, $d\langle v \rangle/dt_{max}/R$, s^{-2}). As necessary for stroke volume calculation, $dZ/dt_{max}/Z_0$ must undergo square root transformation to yield an ohmic mean flow velocity equivalent. To compute SV, the square root of the dimensionless ohmic mean acceleration equivalent ($[dZ/dt_{max}/Z_0]^{0.5}$, s^{-1}) is multiplied by a volume of electrically participating thoracic tissue (V_{EPT}, mL) and left ventricular ejection time (T_{LVE}, s). To find the bulk volume of the thoracic contents (i.e. V_{EPT}), established methods implement exponential functions of measured thoracic length ($L(cm)^n$) or height-based thoracic length equivalents ($0.01 \times \%H(cm)^n$). The new method conceptualizes VEPT as the intrathoracic blood volume (ITBV, mL), which is approximated through allometric equivalents of body mass (aM^b). In contrast to the classical two-element parallel conduction model, the new method comprises a three-compartment model, which incorporates excess extra-vascular lung water (EVLW) as a component of both Z_0 and V_{EPT}. To fully appreciate the evolution and analytical justification for impedance-derived SV equations, a review of the basics of pulsatile blood flow is in order.

Pulsatile Blood Flow

Stroke volume (SV) is defined as that quantity of blood ejected from the cardiac ventricles for each heart beat. More specifically, it relates to the volume of blood ejected from opening to closure of the semilunar valves, and in the case of the left ventricle, the aortic valve. The time interval over which left ventricular ejection occurs is known as left ventricular ejection time (T_{LVE}, s). For purposes of simplicity, and considering this is not an in-depth analytical treatise on pulsatile blood flow, per se, the following simplistic model is proposed as an operational tool for understanding the opposing hypotheses concerning SV determination by means of the transthoracic electrical bioimpedance technique (TEB).

In geometric terms, consider stroke volume V (mL) a cylinder of length S (cm) and cross-sectional area πr^2 (CSA, cm^2). In this model it is assumed that SV is surrounded by a thin-walled viscoelastic aorta, equal in length S to the SV contained within at end-systole. Hemodynamically, as a function of ventricular ejection, let S (cm) also represent the time velocity integral, also known as stroke distance (cm).

$$V = \pi r^2 S \quad \text{(mL)} \tag{1}$$

If the dependent variable, V, and independent variables r and S are continuously differentiable functions of time t, the rate of change of aortic volume dV/dt or flow Q(t) ($mL \cdot s^{-1}$) is given as,

$$\frac{dV(t)}{dt} = \dot{Q} = 2\pi r \frac{dr(t)}{dt} S + \pi r^2 \frac{dS(t)}{dt} \quad (mL \cdot s^{-1}) \tag{2}$$

If $2\pi r S$ (circumference × length) is the internal surface area A_{ISA} (cm^2) of an ascending aortic segment and dr(t)/dt aortic wall velocity ($cm \cdot s^{-1}$), then $\dot{Q}$ (i.e. Q(t)) in derivative 1 equals[1],

---

[1] NB: Q(t) in lieu of $\dot{Q}$ will be used within the body of the text. Whereas Q is the physiologic symbol for volume, Q(t) connotes volume changing with time, which is flow.

$$\dot{Q} = A_{ISA} \times v_{Wall} \quad (\text{mL·s}^{-1}) \tag{3}$$

For derivative 2, if πr^2 is the CSA of the aorta at a discreet point of measurement and $dS(t)/dt$ the axial blood velocity (v, cm·s^{-1}) measured at that point, then axial Q can be given as,

$$\dot{Q} = A_{CSA} \times v_{Blood} \quad (\text{mL·s}^{-1}) \tag{4}$$

Inasmuch as A_{CSA} changes continuously over the cardiac cycle as a function of aortic valve radius dr, the following is an animated representation of derivative 2 of equation 2 and equation 4 [1].

$$\dot{Q} = \int_0^R 2\pi r \frac{dA}{dr} v = \int_0^R 2\pi r dr v \quad (\text{mL·s}^{-1}) \tag{5}$$

At an operational level, derivative 2 of equation 2 and equations 4 and 5 represent the basis for SV determination by means of both the Doppler/echo method and electromagnetic flowmetry. To find SV simply requires integration of the velocity profile over the ejection period at a discreet point in the aortic root and multiplying this by the aortic root CSA at the point of velocity measurement. Common sites for measurement include the left ventricular outflow tract and aortic valve leaflets. Thus,

$$SV = \pi r^2 \int_{t_0}^{t_1} v(t) dt \;\; = \;\; \pi r^2 \times \bar{v} \times t_{LVE} = \pi r^2 S \quad (\text{mL}) \tag{6}$$

where $\bar{v}$ is the mean velocity during ejection and the interval t_0 to t_1, T_{LVE}. Extrapolating derivative 1 of equation 2 and equation 3 for determination of SV is something very much more complex, for it represents the geometric foundation of the *windkessel* model for SV determination [1]. For this model of pulsatile blood flow, it is assumed that the proximal aorta acts as a compliance chamber C and the distal vasculature a static resistance, R_s. Upon the force of ventricular ejection in early systole, and because of distal vascular hindrance, the proximal aorta expands, storing a part of the inflow ($Q(t)_{in}$) as potential energy ($Q(t)_{stored}$). Simultaneously, due to open outflow, blood is expelled axially ($Q(t)_{out}$) to the periphery, where $Q(t)_{out}$ is commonly referred to as "runoff". When aortic pressure exceeds left ventricular pressure from mid-systole to aortic valve closure, the recoiling aorta converts potential energy to kinetic energy, expelling the stored blood to the periphery. From aortic valve closure (end-systole) to end-diastole, non-pulsatile flow dissipates along a quasi-mono-exponential pressure decay. Pulsatile blood flow is therefore buffered and converted from periodic oscillating flow to near-continuous flow for each cardiac cycle [2]. It is this aforementioned physical phenomenon that is the basis for conceptualization of the plethysmographic-based ICG-derived SV equations, and the mechanics underlying the *windkessel* model for pulsatile blood flow. Referring to

derivative 1 of equation 2, if $2\pi r dr / dt$ equals dA/dt (time-rate of change of aortic area, cm^2·s^{-1}), then Q(t) for derivative 1 can be given as,

$$\dot{Q} = \frac{dA}{dt} S = \frac{dV(t)}{dt} \quad (\text{mL·s}^{-1}) \tag{7}$$

In terms of mechanics, since dA(t) and dA(t)/dt are non-linear functions of vessel material composition, pressure P(t) (mmHg) and rate of change of aortic pressure dP(t)/dt (mmHg·s^{-1}), respectively, the following pertains [3]:

$$\frac{dV(t)}{dt} = C \frac{dP(t)}{dt} \quad (\text{mL·s}^{-1}) \tag{8}$$

where the right hand side (rhs) of equation 8 defines the magnitude and shape of the flow wave, and C is the aortic compliance.

If aortic dP(t) is a function of force F and area A, both changing with time over the ejection interval, dP(t) (mmHg) and dP(t)/dt (mmHg · s^{-1}) are given as,

$$dP(t)_{aorta} = \frac{dF(t)}{dA(t)} \Rightarrow \frac{dP(t)_{aorta}}{dt} = \frac{1}{A}\frac{dF(t)}{dt} - \frac{F}{A^2}\frac{dA(t)}{dt} \tag{9}$$

respectively, and compliance C is given as,

$$C = \frac{dA}{dP} S = \frac{dV}{dP} \quad (\text{mL·mmHg}^{-1}) \tag{10}$$

where dA/dP is a non-linear function of Pulse pressure (ΔP) and mean distending pressure P_m. Thus,

$$\frac{dV(t)}{dt} = \frac{dA(P)}{dP} S \frac{dP(t)}{dt} = \frac{dA(P)}{dP} S \left(\frac{1}{A}\frac{dF(t)}{dt} - \frac{F}{A^2}\frac{dA(t)}{dt} \right) =$$
$$\frac{C}{A}\frac{dF(t)}{dt} - \frac{CF}{A^2}\frac{dA(t)}{dt} \quad (\text{mL·s}^{-1}) \tag{11}$$

where the mechanical expression for dV/dt of equation 11 is equivalent to the geometrical definition for dV/dt of derivative 1 in equation 2. As an analytical expansion of equation 8, the rhs of equation 11 more precisely defines the temporal landmarks, shape and magnitude of the radially oriented flow wave.

Figure 1 shows the pressure curve P(t), the rate of change of aortic pressure, dP/dt, aortic blood flow (Q(t)) and the rate of change of flow, which is acceleration of flow, dQ(t)/dt. It is clear from equation 11 that dF/dt_{max}, the major derivative, will occur early in systole, when dA/dt is trivial. Likewise, dA/dt_{max} will occur when dF/dt = 0. When dP/dt is modulated by C, dA/dt_{max} will occur at the peak magnitude of the flow wave dV/dt_{max} (i.e. Q_{max}) and dF/dt_{max} will occur on the steepest portion of the flow wave,

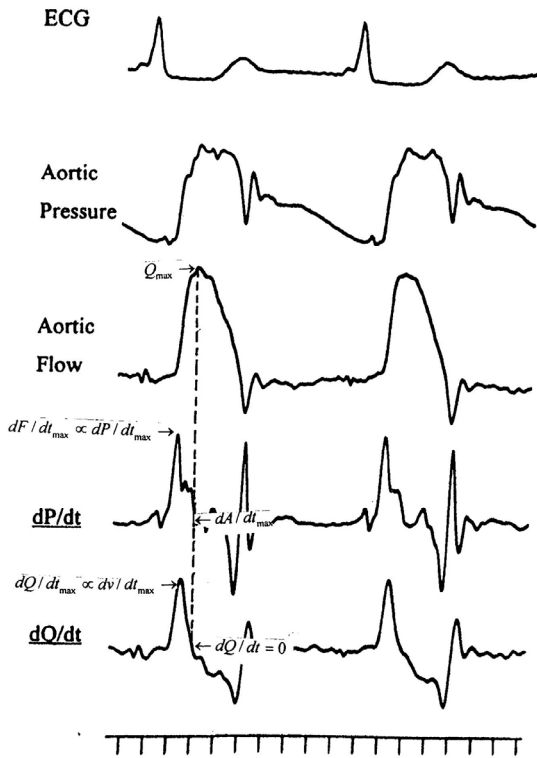immediately following aortic valve opening in early systole.

Fig. 1. ECG, aortic pressure, aortic blood flow Q, aortic rate of change of pressure dP/dt, and rate of change of flow, which is acceleration dQ/dt. From a canine model In: Li J-K. The arterial circulation: physical principles and clinical applications. Totowa, NJ: Humana Press; 2000, p. 78.

When flow is differentiated with respect to time dQ/dt_{max} will occur when dA/dt and dV/dt are minimal. Also apparent is that when flow acceleration = 0, dV/dt is at maximum. Therefore, $dQ(t)/dt_{max}$ and dV/dt_{max} are monotonically restricted to their respective time-domains, with acceleration of blood flow, dQ/dt_{max} peaking, on the mean, approximately 50ms before peak flow, dV/dt_{max}.

If S is a segment of aorta with closed outflow, then flow into the segment would be the total input flow from left ventricular ejection. If, however, segment S is an open outflow conduit, equation 8 would represent a net flow. For a simple 2-element *windkessel* model, net flow into the segment ($Q(t)_{in}$) is given as [4],

$$\dot{Q}_{in-net} = C\frac{dP(t)}{dt} - \frac{P(t)}{R_s} \quad (\text{mL}\cdot\text{s}^{-1}) \qquad (12)$$

where derivatives 1 and 2 on the rhs of (12) represent $Q(t)_{stored}$ and $Q(t)_{out}$, respectively.

To obtain total flow $Q(t)_{total}$ through the segment over a single systolic interval (T_{LVE}, s), $Q(t)_{out}$ must be measured. With regard to a two-element *windkessel* model, $Q(t)_{out}$ is obtained by dividing the pressure change over the ejection interval P(t) by the distal, or systemic vascular resistance,

R_s. R_s is defined as the quotient of mean pressure to mean flow P_m/Q_m. $Q(t)_{total}$ is thus given as [4],

$$\dot{Q}_{in-total} = C\frac{dP(t)}{dt} + \frac{P(t)}{R_s} \quad (\text{mL}\cdot\text{s}^{-1}) \qquad (13)$$

Integration of $Q(t)_{strored}$ yields stored volume inflow, SV_{stored}:

$$SV_{stored} = C\int_{t_0}^{t_1}\frac{dP(t)}{dt}dt = C\Delta P \qquad (\text{mL}) \qquad (14)$$

where ΔP is the pulse pressure, which is aortic peak systolic pressure P_s minus aortic diastolic pressure P_d (P_s–P_d) [5].

Since SV = $C\Delta P$, where C is a non-constant time variable function of pressure P, the following expression also represents total flow into a segment of aorta of length S and internal surface area wall velocity dA/dt [6].

$$\dot{Q}_{in} = C\frac{dP(t)}{dt} + P\frac{dC_P(t)}{dt} \quad \left(\text{mL}\cdot\text{s}^{-1}\right) \qquad (15)$$

where derivatives 1 and 2 represent $Q(t)_{stored}$ and $Q(t)_{out}$, respectively. Differentiating $dC_p(t)/dt$ results in,

$$\frac{dC_p(t)}{dt} = \frac{d\left(\frac{\Delta V}{\Delta P}\right)}{dt} = \frac{1}{P}\frac{dV}{dt} - \frac{V}{P^2}\frac{dP}{dt} \qquad (16)$$

In terms of total flow into segment S, equations 12 and 15 are equivalent. Integration of equation 13 over an ejection interval yields SV and is thus given as [2],

$$SV = \int_{t_0}^{t_1}\dot{Q}(t)dt = C\int_{t_0}^{t_1}\frac{dP(t)}{dt}dt + \frac{1}{R_s}\int_{t_0}^{t_1}P(t)dt \qquad (17)$$

where equation 17 represents a two-element *windkessel* model. Derivatives 1 and 2 on the rhs equation 17 represent V_{stored} and V_{out}, respectively.

Although a theoretically correct model for SV, equation 17 is not easily solved. Clearly, P(t), dP(t)/dt, and P_m can be computed by direct measurement and signal processing, but C and R_s must be obtained independently by alternative means [2]. This is clear from equation 10 for the determination of C and the relationship of R_s to $Q(t)_{mean}$ in equation 17. From equations 15 and 16, it is also clear that C is not a constant as equation 17 implies. Pressure dependent C and the rate of change of C with respect to time, dC/dt, are not accounted for in equation 17. To more accurately predict SV from the *windkessel* model, it is necessary to incorporate the transverse frequency-dependent pulsatile resistance, also known as mechanical or characteristic aortic input impedance, Z_c. Z_c is approximated by aortic pulse pressure divided by peak aortic blood flow ($\Delta P/Q_{max}$). Incorporating characteristic aortic impe-

dance into the *windkessel* model, which constitutes the three-element model, is now considered the "gold-standard" [4]. Thus, as an approximate unifying statement for SV from equations 5, 6 and 17:

$$SV = \int_0^R 2\pi r dr \int_{t_0}^{t_1} v(t) dt = \pi r^2 S \cong C \int_{t_0}^{t_1} \frac{dP(t)}{dt} dt + \frac{1}{R_s} \int_{t_0}^{t_1} P(t) dt$$

(mL)   (18)

Impedance Cardiography

Modeling the transthoracic impedance Z(t)

Impedance cardiography (ICG) is a branch of bioimpedance primarily concerned with the determination of left ventricular stroke volume (SV) [7–10]. It was the first and still the only truly noninvasive, continuous, operator-independent, hands-off, beat-to-beat method used in clinical practice. Despite these desirable attributes, general acceptance of the method as a replacement for invasive reference standards in critically-ill humans has not been realized. As summarized by Raaijmakers et al. and Moshkovitz et al., both correlation and agreement against standard reference methods have been far too variable to reliably apply the method clinically for modulation of patient therapy [7,12]. As emphasized by Kauppinen et al. [11], the major problem in cardiovascular impedance measurements is the inability to accurately correlate the magnitude of the impedance waveforms to the hemodynamic variables they pretend to mimic. The lack of consistently high correlation and agreement between ICG measurements and reference standards would suggest that, the equation models describing SV in ICG are not sufficiently robust and the physical acquisition of the impedance signals not sensitive and specific enough for clinical application in the critically ill [11].

While measurements can be obtained by the whole body technique, the method is usually implemented by means of the transthoracic approach (i.e. transthoracic electrical bioimpedance cardiography, TEB, ICG) [7]. The latter technique, and subject of this review, involves applying a current field longitudinally across a segment L (cm) of thorax by means of a constant magnitude, high frequency (50–100 kHz), low amplitude AC (I(t)) (1–4 mA). By Ohm's Law, the voltage difference U(t) (volt, U) measured within the current field is proportional to the transthoracic electrical impedance Z.

$$\frac{U(t)}{I(t)} = Z \quad (\Omega)$$

(19)

where Z is the frequency-dependent AC analog of the static DC resistance R. The magnitude of the impedance, or modulus, $|Z|$, comprises a resistive component, also known as the real part, R, and an imaginary part X. X is further comprised of an inductive part (X_L) and capacitive

part (X_C), both collectively known as the reactance. With regard to the magnitude of X, X_L is proportional and X_C inversely proportional (1/f) to the frequency of the applied AC. $|Z|$ is determined by the geometric addition of the resistive and reactive components.

$$|Z| = \sqrt{R^2 + (X_L - X_C)^2}$$

(20)

where the reactance X is,

$$X = (X_L - X_C)$$

(21)

Thus,

$$|Z| = \sqrt{R^2 + X^2}$$

(22)

where the magnitudes of R and X on Cartesian coordinates are determined by the phase angle φ, and thus, R *tan* φ = X. For the remainder of the discussion, let $|Z| = Z$.

For cylindrical electrical conductors, and as a companion equation to equation 19 [13],

$$Z = \frac{\rho L}{A} \equiv \frac{\rho L^2}{V} \quad (\Omega)$$

(23)

where ρ = the resistivity (Ω·cm), L = the length of the conductor, and A and V are the CSA (cm²) and volume (mL) of the conductor, respectively. Thus, substituting ρL²/V in equation 23 for Z in equation (19) and rearranging,[2]

$$I(t) \cdot \frac{\rho L^2}{V} = U(t) \quad (U)$$

(24)

If the thorax is considered a cylindrical bulk electrical conductor of length L between the voltage sensing electrodes, with ρ_T the transthoracic specific resistance and V_T the volume of thorax, then, without ventilatory or cardiac activity, Z in equations 19 and 23 represents the adynamic or static transthoracic base impedance Z_0. When cardiac and ventilatory activity are superimposed on Z_0, a time-variable transthoracic impedance is registered, Z(t). By eliminating the oscillating cardiac-asynchronous ventilatory component ΔZ_{vent}, Z(t) comprises, in parallel, a static DC component Z_0 (22Ω–45Ω) and a dynamic AC component $\Delta Z(t)$ (0.1Ω–0.2Ω) [14,15] (Fig.2). It should be noted that the magnitude of Z_0 not only varies between individuals and the frequency of the applied AC, but also with the electrode configuration used for signal acquisition. For four common electrode configurations a computer model predicts a Z_0 range of 26.3Ω–34.3Ω [11].

---

[2] For the remainder of the discussion, the character "U" is used in *lieu* of "v" for volt, so as not to confuse v with velocity "*v*" or volume "V".

When electrical resistances or impedances are added in parallel, they are summed as their reciprocals.

$$Z(t) = Z_0 \| \Delta Z(t) = \frac{1}{Z(t)} = \frac{1}{Z_0} + \frac{1}{\Delta Z(t)} \qquad (25)$$

As a composite impedance with tissues of widely varying specific resistances, Z_0 comprises, in parallel, a static, relatively non-conductive multi-compartmental tissue impedance Z_t ($400\Omega\cdot cm-10^{20}\Omega\cdot cm$) [11,16], a highly conductive blood impedance Z_b (or resistance R_b $100\Omega\cdot cm-180\Omega\cdot cm$) varying with hematocrit [17], and a very highly conductive interstitial extra-vascular lung water (EVLW) impedance Z_e ($60\Omega\cdot cm-70\Omega\cdot cm$).
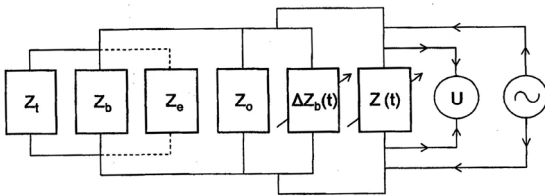

Fig. 2. Schematic of a multi-compartmental parallel conduction model of the thorax. The transthoracic electrical impedance $Z(t)$ to an applied AC field represents the parallel connection of a quasi-static base impedance Z_0 and a time-dependent component of the blood impedance, $\Delta Z_b(t)$. Z_0 represents the parallel connection of all static tissue impedances, Z_t, and the static component of the blood resistance, Z_b. Z_e represents the quasi-static EVLW compartment. A voltmeter (U) and AC generator (~) are shown. From reference 37.

Z_0 is thus an intensity weighted mean of the reciprocal sum of all thoracic tissue impedances, the sum of the reciprocals being less than the lowest tissue impedance of the thorax.

$$Z_0 = Z_t \| Z_b \| Z_e = \frac{1}{Z_0} = \frac{1}{Z_t} + \frac{1}{Z_b} + \frac{1}{Z_e} \qquad (26)$$

In this model, the blood resistance R_b is considered a cylindrical tube of constant length L, surrounded by the highly conductive extravascular lung water impedance Z_e and both surrounded by a non-conductive thoracic encompassing cylinder Z_t. It should be noted that, at the frequencies used in ICG, blood is almost purely resistive with a trivial reactive component. Therefore, the term blood resistance, R_b, is justifiably used in lieu of blood impedance Z_b.

$\Delta Z_b(t)$: The Transthoracic Cardiogenic Impedance Pulse Variation

The velocity and volume components

The systolic portion of the cardiogenically-induced impedance pulse variation $\Delta Z(t)$, hereafter known as $\Delta Z_b(t)$, comprises two components, arguably of equal magnitude [14,18–21]. The first is a velocity-induced change in the specific resistance of axially directed flowing blood ($\Delta\rho_b(t)$,

$\Omega\cdot cm\cdot s^{-1}$), where, in end-diastole, the state of highest blood resistivity, red blood cells are randomly oriented. By contrast, during peak aortic blood acceleration and the rapid ejection phase of early systole, red blood cells become deformed and assume a well defined state of parallel orientation along their long axis of symmetry [19,22,23] (fig. 3).
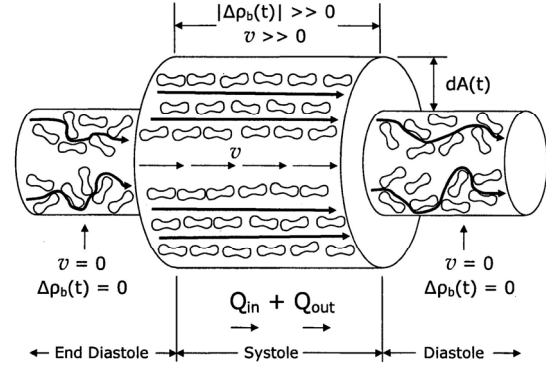

Fig. 3. Behavior of AC as applied to pulsatile blood flow. → = AC flow. v = red cell velocity; $\Delta\rho_b(t)$ = changing specific resistance of flowing blood.; Q_{in} = flow into aortic segment; Q_{out} = simultaneous flow out of aortic segment; $dA(t)$ = time-dependent change in aortic CSA. From reference 13.

Parallel alignment opens clear current pathways through the highly conductive plasma, causing a decrease in blood resistivity and transthoracic resistivity [19,22] (i.e.↑Conductivity). The rapidity of and degree to which attainment of complete parallel orientation is achieved determines the magnitude of the resistivity change $\Delta\rho_b(t)_{max}$ ($\Omega\cdot cm\cdot s^{-1}$) [23]. The maximum resistivity change occurs when the long axis of the red cell is oriented within 20^0 to the direction of blood flow [23]. Figure 4 shows that, in early ejection, maximum acceleration of red cell reduced average velocity (i.e. mean spatial velocity) parallels the change in blood resistivity (i.e. conductivity) (r = 0.99). By comparison, upon negative acceleration, the resistivity change does not parallel the reduced average velocity, with subsequent delay in reaching baseline [19,23]. This disparity is, no doubt, a consequence of the red cells' inability to achieve complete randomization at end-systole.
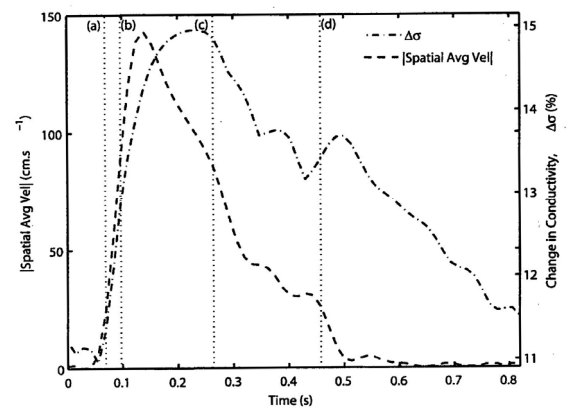

Fig. 4. Absolute spatial average velocity (i.e. reduced average velocity $<v>/R$, s^{-1}) vs. conductivity change in an *in vitro* pulsatile ejection model over one cardiac cycle. Note that, upon red cell acceleration in early ejection, the peak rate of change of the reduced average velocity parallels the peak rate of change of conductivity (r = 0.99). From reference 23.

The second component generating a change in transthoracic specific resistance is the transversely or laterally-oriented volume displacement of non-conductive alveolar gas ($\rho = 10^{20}$ $\Omega \cdot$cm) by stroke volume-induced expansion of the ascending aorta, principally [24,25], with highly conductive blood ($\rho_b = 100–180$ $\Omega \cdot$cm) $\Delta V_b(t)$ ($\Delta \Omega \cdot$cm(t)). As discussed under pulsatile blood flow, in addition to distal vascular hindrance R_s, the volumetric expansion of the aorta is due to pressure-induced, compliance modulated changes in cross sectional area, πr^2 (cm^2), and, over segment L, a change in internal surface area, $2\pi \cdot$(dA/dr)L, (cm^2) [1,26]. For example, assume that equation 23 represents the impedance Z of a segment of very thin walled aorta embedded within the thorax. Assume that the aortic segment is of length L with open outflow, the content of which is blood of static specific resistance ρ_b and volume V_b. Thus, an increase in aortic volume $\Delta V_b(t)$ would result in a corresponding decrease in vessel and transthoracic impedance $\Delta Z_b(t)_{volume}$.

$$\downarrow \Delta Z_b(t)_{volume} = \frac{\rho_b L^2}{\uparrow \Delta V_b(t)}(\Delta \Omega(t))$$

$$\Rightarrow \uparrow \Delta V_b(t) = \frac{\rho_b L^2}{\downarrow \Delta Z_b(t)} \quad (\Delta volume(t)) \qquad (27)$$

where the rhs of equation 27 is the ohmic equivalent of equation 14, wherein $\Delta Z_b(t)$ and $\Delta V_b(t)$ represent net changes. The combined velocity and volume effects cause a steep drop in transthoracic impedance.

For the velocity-induced change in blood resistivity, the decrease in vessel and transthoracic impedance is given as,

$$\Delta Z_b(t)_{velocity} = \frac{\Delta \rho_b(t)L^2}{V_b} \quad (\Omega \cdot s^{-1}) \qquad (28)$$

where $\Delta \rho_b(t)$ is of diminishing value upon ejection. Combining equations 27 and 28,

$$\Delta Z_b(t) = \frac{\Delta \rho_b(t)L^2}{V_b} + \frac{\rho_b L^2}{\Delta V_b(t)} = \Delta Z_b(t)_{velocity} + \Delta Z_b(t)_{volume} \ (29)$$

Combining equations 24, 26, and 29, the following impedance model describes the static and dynamic impedances in parallel, when an AC field is applied longitudinally across the thorax (fig 2).

$$I(t)\left[\left(\|Z_t\|Z_b\|Z_e\right)\|\left(\Delta Z_b(t)_{velocity} + \Delta Z_b(t)_{volume}\right)\right] + U_0 + \Delta U_b(t) \ (30)$$

Stroke Volume Equations

Nyboer equations: Foundation and Rationale for the Plethysmographic Hypothesis and Parallel Conduction Model in Impedance Cardiography

The original Nyboer equation [27] was specifically proposed for determination of segmental blood volume changes in the upper and lower extremities. It is based upon the assumption that the arteries of the extremities are rigidly encased in muscle and connective tissue, and that both the arteries and surrounding tissue can be approximated as cylindrical conductors placed in parallel alignment. Nyboer found that, by placing spaced-apart circumferential current injecting electrodes on a limb segment and voltage sensing electrodes within the current field proximate the current injectors, impedance changes proportional to strain gauge determined blood volume changes could be measured. He also determined that, in order to compensate for simultaneous volume outflow from the limb segment during arterial inflow, venous outflow occlusion was necessary. Thus, the $\Delta Z_b(t)$ waveform represents the sum of two signals: one caused by inflow and the other caused by outflow (runoff) between the voltage sensing electrodes [28]. Using venous outflow obstruction, absolute volume changes during each pressure pulse were accurately approximated. Nyboer referred to this method, and quite accurately as, electrical impedance plethysmography. The foundation of Nyboer's equation, and for that matter the earliest SV equations, originate from equation 27, where, when solving for $\Delta V_b(t)_{net}$,

$$\Delta V_b(t)_{net} = \frac{\rho_b L^2}{\Delta Z_b(t)_{net}} \quad (\text{ mL}) \qquad (31)$$

However, since a large extremity artery (i.e. brachial or femoral) is encased in muscle and connective tissue, $\Delta Z_b(t)$ had to be further refined, reflecting a parallel connection of the static tissue and dynamic blood impedances. Since the magnitude of Z(t) of an extremity is larger than extremity Z_0 by a trivial factor of extremity $\Delta Z_b(t)$, the approximation that extremity Z(t) and Z_0 are virtually identical is a plausible assumption. Without assumption, it also follows that Z(t)–Z_0 = $\Delta Z_b(t)$. Thus, if equation 25 is solved for $\Delta Z_b(t)$, using the reciprocal rule for impedances added in parallel:

$$\Delta Z_b(t) = \frac{Z_0 \cdot Z(t)}{Z_0 - Z(t)} \cong \frac{Z_0^2}{-\Delta Z_b(t)} \quad (\Omega(t)) \qquad (32)$$

Substituting the right hand side of equation 32 for $\Delta Z_b(t)$ into equation 31 results in the operational model for measurement of blood volume changes in an extremity. For the maximum volume change $\Delta V_{b(max)}$ with venous outflow occlusion [28],

$$\Delta V_{b(\max)} = -\frac{\rho_b L^2}{Z_0^{\,2}} \Delta Z_{\max} \quad \text{(mL)} \qquad (33)$$

where $\Delta Z_{\max}$ is the peak magnitude of the waveform and $\rho_b L^2/Z_0^{\,2}$ is a constant. For an arterial conduit with closed outflow, equation 33 is the bioelectric equivalent of the hemodynamic expression given for SV in equation 14 with outflow obstruction. For an extremity vessel with open outflow, equation 33 is analogous to the integrated value for equation 12. Clearly, as applied to SV calculations, equation 33 is inadequate, because complete aortic outflow obstruction for calculation of total SV is impossible.

Stroke Volume Calculation

Nyboer's method: Maximum Systolic Down-slope Backward Extrapolation of $\Delta Z_b(t)$.

As applied to thoracic measurements of SV, Nyboer professed to have solved the outflow problem by manually determining the maximum systolic down-slope of $\Delta Z_b(t)$ and extrapolating it backward to the beginning of ejection [28]. Thus, the maximum impedance change resulting from the backward extrapolation method was believed to be equivalent to the maximum impedance change attained as if no arterial runoff occurred during ejection.
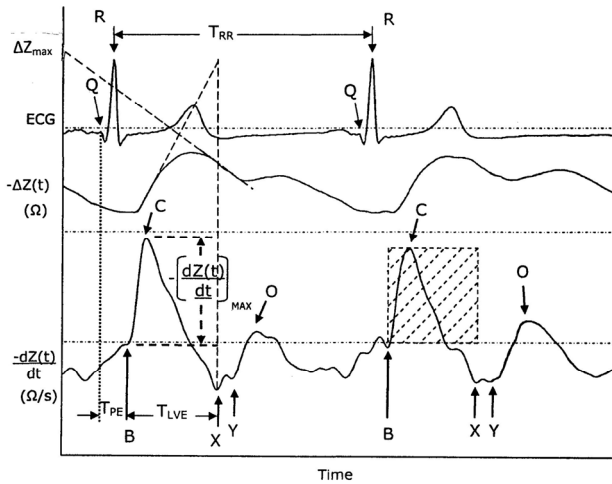

Fig. 5. ECG, $\Delta Z(t)$ and dZ/dt waveforms from a human subject. For $\Delta Z(t)$ note Nyboer's maximum down-slope backward extrapolation to find $\Delta Z_{\max}$. Also note Kubicek's maximal systolic up-slope forward extrapolation of $\Delta Z(t)$. For dZ/dt, point B = aortic valve opening; point X = aortic valve closure; Y = pulmonic valve closure; O = rapid ventricular filling wave; Q–B interval = pre-ejection period (s); B–C interval = time-to-peak (TTP, s) of dZ/dt$_{\max}$; B–X interval; left ventricular ejection time (T_{LVE}, s). dZ/dt waveform to right shows the square wave integration (shaded area), dZ/dt$_{\max}$ remaining constant over the ejection interval, which represents outflow compensation. Modified from reference 13.

Thus, SV, or the maximum volume change ΔV_b measured between the voltage sensing electrodes is given as,

where Z_0 is the static transthoracic base impedance and $\Delta Z_{\max}$ is the maximum backward extrapolated value of the thoracic cardiogenic impedance pulse variation, which includes runoff. While credible SV values could be obtained with equation 34, it was not widely accepted, this being due to difficulty in manually determining the true maximum downslope.

Kubicek's Method: Maximum Systolic Upslope Forward Extrapolation of $\Delta Z_b(t)$

As a consequence of the deficiencies of the backward extrapolation procedure, Kubicek et al. proposed a maximum systolic forward extrapolation of $\Delta Z_b(t)$, which is the basis for all subsequent plethysmographic conceptually-based SV equations using the transthoracic approach [29,30]. Kubicek et al. made the assumption that, if the maximum systolic upslope (i.e. $\Delta Z' = \Delta Z \cdot s^{-1}$, $\Omega \cdot s^{-1}$) is held constant throughout ejection, then compensation for outflow, before and after attainment of $Q_{\max}$ is achieved. Theory underlying Kubicek's method assumes that little arterial runoff occurs during the inertial phase of rapid systolic ejection. Unlike Nyboer's direct measurement of $\Delta Z_{\max}$, Kubicek's method requires multiplying $\Delta Z'$ (forward extrapolation) by left ventricular ejection time T_{LVE} (i.e. $\Delta Z' \times T_{LVE} = \Delta Z_{\max}$). In the original description of the technique, T_{LVE} was determined by means of phono-cardiography. As opposed to manual extrapolation of $\Delta Z'$, electronic differentiation of $\Delta Z_b(t)$ was implemented. The first time-derivative clearly defines dZ/dt$_{\max}$, with the presumed units of $\Omega \cdot s^{-1}$, as a distinct point C and left ventricular ejection time (s) as the interval between points B (aortic valve opening) and X (aortic valve closure) (fig. 5). Thus, $\Delta Z_{\max} = $ dZ/dt$_{\max} \times T_{LVE} = \Omega$. Kubicek's equation is thus obtained by substituting dZ/dt$_{\max} \times T_{LVE}$ for $\Delta Z_{\max}$ in equation 34. The Kubicek equation is given below and purportedly equivalent to equation 17. Thus [29,30],

$$SV_{Kubicek} = \frac{\rho_b L^2}{Z_0^{\,2}} \frac{dZ(t)}{dt_{\max}} T_{LVE} \quad \text{(mL)} \qquad (35)$$

where ρ_b is the static specific resistance of blood, which was initially fixed at 150 $\Omega \cdot$cm [29]. As concerns the appropriate value for ρ, Quail et al [31] rearranged the Kubicek equation (assuming it correct), solved for ρ as the dependent variable, and measured SV by EMF. By means of normovolemic hemodilution exchange transfusion, they showed that, over a wide range of hematocrit from 26%–66%, the value of ρ remained virtually constant about a mean of 135$\Omega \cdot$cm at hematocrit 40%. L (cm) is the longitudinal distance between the voltage sensing electrodes on the base of the neck and those on the lower thorax at the level of the xiphoid process. Z_0 is the quasi-

static base impedance measured between the voltage sensing electrodes. In an in vitro expansible tube model, when equation 35 is compared to equation 33 without outflow occlusion, equation 33 systematically underestimates SV obtained from 35 [26]. By elimination of a Z_0 term, the volume conductor V_C in equation 35 is given as,

$$V_C = \frac{\rho_b L^2}{Z_0} \quad \text{(mL)} \qquad (36)$$

where, when Z_0 varies with alterations in extravascular lung water, the V_C is non-constant. Equation 35 is, in theory, modeled as the ohmic equivalent of *windkessel* equation 17, where outflow correction is explicitly defined. Thus, by analogy and inspection of equation 17, Kubicek's equation is conceptually and explicitly dependent on aortic pressure, the rate of change of aortic pressure and mean arterial pressure. However, by comparison with equation 17, and without theoretical or mathematical explanation, Kubicek's equation implicitly integrates the unknowns of compliance C, characteristic (mechanical) aortic input impedance (Z_c) and systemic vascular resistance R_s into the overall theoretical gestalt.

Assumptions of the Nyboer/Kubicek method [14,15]:

1. The transthoracic impedance Z(t) is considered the parallel connection of an aggregate of static cylindrical tissue impedances, Z_t, considered as one, and, encased within, a dynamic blood resistance, R_b, otherwise known as the blood impedance, Z_b.

2. The blood resistance is considered a homogeneously conducting blood-filled cylinder of constant length L, or a parallel connection of an aggregate of cylinders considered as one.

3. The current distribution in the blood resistance is uniform.

4. All current flows through the blood resistance.

5. The volume conductor V_C is homogeneously perfused with blood of specific resistance ρ_b.

6. The magnitude of stroke volume is directly proportional to power functions of measured distance L between the voltage sensing electrodes [29–30], or to height-based thoracic length equivalents [32].

7. All pulsatile impedance changes $\Delta Z_b(t)$ are due to vessel volume changes $\Delta V_b(t)$, and, in the context of assumption 2, $\Delta Z_b(t)$ is due exclusively to changes in vessel radius dr(t) and CSA dA(t).

8. In the context of assumption 7, dZ/dt_{max} is the bioelectric equivalent of dV/dt_{max}, $\dot{Q}_{max}$

(i.e. $\frac{dA(t)}{dt_{max}} \times L = \frac{dV(t)}{dt_{max}}$). See equation 7.

9. Outflow, or runoff during ventricular ejection, can be compensated for by extrapolating the peak rate of change of $\Delta Z_b(t)$ over the ejection interval (i.e. $dZ/dt_{max} \times T_{LVE}$) to obtain ΔZ_{max} [29–30].

10. The specific resistance (resistivity) of blood ρ_b is constant during ejection [29]

11. The transthoracic specific resistance, ρ_T, is constant [31].

Sramek-Bernstein Method: A Constant-Magnitude Volume of Electrically Participating Thoracic Tissue V_{EPT}

The assumptions of the Sramek-Bernstein equation are virtually identical to those of the Kubicek method, except for the physical definition and magnitude of the V_C [32]. In Sramek's interpretation of Kubicek's V_C, ρ and a Z_0 variable are eliminated by mathematical substitution. This simplification assumes, as per the work of Quail et al. [29] that, the ρ_T equivalent, Z_0A/L can replace ρ_T. By this substitution, V_C is rendered a personal constant for each individual. Sramek [32] named the modification of Kubicek's V_C as the volume of electrically participating thoracic tissue, V_{EPT}. Conceptually, as opposed to Kubicek's cylindrical V_C, Sramek's V_{EPT} is geometrically a frustum, or truncated cone. Full mathematical derivation and justification for Sramek's model is provided elsewhere [32]. The original Sramek equation is given as,

$$SV_{Sramek} = V_{EPT} \frac{dZ/dt_{max}}{Z_0} T_{LVE} = \frac{L^3}{4.25} \frac{dZ/dt_{max}}{Z_0} T_{LVE}$$
$$\text{(mL)} \quad (37)$$

where L is the measured distance (cm) between the voltage sensing electrodes and 4.25 an experimentally-derived constant. The Bernstein modification of V_{EPT} assumes that SV is not only a function of thoracic length, but also body weight and blood volume. Correcting for the magnitude of the blood resistance (i.e. intrathoracic blood volume, ITBV, mL) and using the work of Feldschuh and Enson [33], a factor δ (delta) was appended to the Sramek equation. The Sramek-Bernstein equation is given as [32],

$$SV_{S-B} = \delta \frac{L^3}{4.25} \frac{dZ/dt_{max}}{Z_0} T_{LVE} \quad \text{(mL)} \qquad (38)$$

where L is a thoracic length equivalent, equal to 17% of body height (i.e. 0.17·H) (cm), and delta δ is the weight correction for blood volume. δ is a dimensionless parameter, which corrects for deviation from ideal body weight (kg) at any given height and further modified for the indexed blood volume (mL·kg^{-1}) at that weight deviation [32,33].

Validity of the Plethysmographic Hypothesis and its Assumptions:

In order for equations 35, 37 and 38 to yield equivalent results to equation 17, it must be demonstrated that dZ/dt_{max} is explicitly dependent on aortic systolic pressure P(t), the rate of change of aortic pressure dP/dt, mean arterial pressure P_{mean}, systemic vascular resistance R_s and aortic compliance C. In an early, well designed experimental study, Yamakoshi et al. [1] demonstrated that, in an *in vitro* distensible tube model, the magnitude of impedance-derived SV is not related to any one of the above *windkessel* parameters. Despite their results, which clearly invalidate the plethysmographic hypothesis, the literature has ignored these findings. Data provided by Djordjevich et al. [34], though purporting to show a close relationship between dZ/dt_{max} and blood pressure levels, actually demonstrated that the correlations are weak, at best. Clinically, Brown et al. [35] demonstrated that, despite advancing age (20–80 years) and progressive stiffening of the aorta, ICG CO is nonetheless highly correlated with thermodilution CO (TDCO). It is also interesting to note that, as an alleged analog of dV/dt_{max}, dZ/dt_{max} supposedly provides an ohmic mean velocity analog necessary for SV calculation (*vide infra*). As concerns the volume conductor (V_{EPT}) of the Kubicek equation (equation 36), it seems quite improbable that the transthoracic specific resistance, ρ_T, remains constant in the face of changing values of Z_0. By inspection of equation 23, L and V remaining constant, it is apparent that this is impossibility, because, ρ_T must vary directionally with its dependent variable Z_0. Other unanswered questions concerning the validity of the plethysmographic hypotheses include the following:

1. The proper value, physiologic definition, and theoretical basis for ρ: i.e. does ρ vary with hematocrit (ρ_b), or is it a constant based on thoracic resistivity (ρ_T)?

2. The physiological relevance of measured L or thoracic length equivalents in the Kubicek and Sramek-Bernstein equations regarding SV.

3. The validity of the outflow extrapolation procedure [36].

4. A coherent physiologic basis and correlate for the empirically-derived volume conductors and their relevance to SV.

5. Lack of consideration for the changing transthoracic base impedance (ΔZ_0) in critical illness, typified by increased thoracic liquids (pulmonary edema) causing aberrant electrical conduction [37].

6. Lack of regard for the effect of the blood velocity-induced change in the transthoracic specific resistance $\Delta\rho_b(t)$ [37].

7. Origin of dZ/dt_{max} in the hemodynamic time domain [37].

Despite the objections to the plethysmographic hypothesis, correlation with reference standards is considered good ($r^2 = 0.67$, range = 0.52–0.81 and, r = 0.82, range = 0.70–0.90 [7,12]. However, high correlation and reasonable agreement with invasive reference standards does not verify the plethysmographic hypothesis as correct. It may simply mean that the product of dZ/dt_{max}, T_{LVE}, and a best-fit volume conductor V_C, yield results that mimic reference method SV [14,15].

Origin of dZ/dt_{max}

Resolution of Origin by Differential Time-Domain Analysis

If equation 23 is differentiated by parts with respect to time, the following results:

$$\frac{dZ(t)}{dt} = \frac{dZ_{length}(t)}{dt} + \frac{dZ_{vel}(t)}{dt} - \frac{dZ_{vol}(t)}{dt} \quad (39)$$

Furthermore, if all variables in equation 23 are continuously differentiable functions of time and are expressed within the respective dZ/dt derivatives of equation 39 [37],

$$\frac{dZ(t)}{dt} = \frac{\rho_b}{V_b}\frac{2L}{1}\frac{dL(t)}{dt} + \frac{L^2}{V_b}\frac{d\rho_b(t)}{dt} - \frac{\rho_b L^2}{V_b^2}\frac{dV_b(t)}{dt} \quad (40)$$

Since dL and dL/dt are of trivial magnitude, dZ/dt comprises derivatives 2 and 3, the units of which are $\Omega\cdot s^{-2}$ and $\Omega\cdot s^{-1}$, respectively.

Using older plethysmographic techniques, which are conceptually analogous to the simple two-element *windkessel* model, simultaneous outflow during inflow over aortic segment L is compensated for by using the maximal systolic upslope extrapolation of $\Delta Z_b(t)$. The peak slope is conceptually believed to be the peak slope of $\Delta Z_{vol}(t)$, and, according to theoretical assumptions, represents the ohmic equivalent of the peak rate of change of aortic volume (peak flow, dV/dt_{max}, $mL\cdot s^{-1}$), at and before which little outflow is thought to occur [36]. When extrapolated over the ejection interval, this convention is believed to be proportional to total SV [29,30]. To better define the peak slope, $\Delta Z_b(t)$ is electronically differentiated to dZ/dt (i.e. $d[\Delta Z_b(t)]/dt$), the peak magnitude of which is dZ/dt_{max} and conceptually analogous to the peak value of derivative 3 of equation 40 (i.e. $d[\Delta Z_{vol}(t)]/dt_{max}$). That is,

$$\frac{dZ_{vol}(t)}{dt_{max}} = \frac{\rho_b L^2}{V_b^2}\frac{dV_b(t)}{dt_{max}} \quad (\Omega\cdot s^{-1}) \quad (41)$$

A recently introduced ICG method conceptualizes the peak value of derivative 2 of equation 40 to represent

dZ/dt_{max}, which is the peak rate of change of the red cell velocity-induced blood resistivity variation $d\rho_b(t)/dt_{max}$ $(\Omega \cdot cm \cdot s^{-2})$ (i.e $d[\Delta Z_{vel}(t)]/dt_{max}$, $\Omega \cdot s^{-2}$) [37]. Thus,

$$\frac{dZ_{vel}(t)}{dt_{max}} = \frac{L^2}{V_b} \frac{d\rho_b(t)}{dt_{max}} \quad (\Omega \cdot s^{-2}) \qquad (42)$$

While differential time domain analysis provides the two possible origins of dZ/dt_{max}, the definitive origin requires temporal correspondence of dZ/dt_{max} with either peak ascending aortic blood flow $(Q(t)_{max}, dV/dt_{max})$ or peak aortic blood acceleration $(dv/dt_{max}, dQ/dt_{max})$.

Resolution of Origin by Comparative Time-Domain Analysis: Evidence for a New Paradigm

Comparative time domain analysis confirms that peak flow velocity occurs at ~ 100±20ms after opening of the aortic valve [38], whereas dZ/dt, (as extrapolated from the data of Matsuda et al. [39] and Lozano et al. [40]) and acceleration dv/dt peak at a mean value of 50 (Lozano)→60 (Matsuda)±20ms. As testaments to the validity of these rise times, which is the temporal interval between aortic valve opening, designated as point B on the dZ/dt tracing to dZ/dt_{max}, data provided by Matsuda et al. [39] show that, when the time interval from the Q wave of the ECG to $LVdP/dt_{max}$ is subtracted from the time interval between the Q wave and dZ/dt_{max}, TTP of dZ/dt_{max} = 60±15ms (i.e. $[Q→dZ/dt_{max}(ms)] - [Q→LVdP/dt_{max} (ms)] = 60±15$ ms). This analysis is valid, because, in the absence of aortic valve disease, $LVdP/dt_{max}$ almost invariably occurs within 2–5 ms just prior to aortic valve opening. Corroborative evidence from Lozano et al., obtained by subtracting the R(ECG)→B(dZ/dt) interval (mean 68 ms, range 47–84 ms) from the R→dZ/dt_{max} interval (mean 120ms, range 80–160ms), shows that the mean rise time (TTP) from point B to dZ/dt_{max} = 52±20 ms (i.e. [R→dZ/dt_{max} ms] – [R→B ms] = 52±20 ms). These calculated rise times are corroborated by actual measurements obtained by Debski et al. [41]. It can also be shown that TTP of both dv/dt and dZ/dt occur in the first 10–20% of systole, whereas peak flow velocity occurs at the end of the first third of systole [13]. Matsuda et al. have shown that, while peaking out of phase, the maximum upslope and TTP of $LVdP/dt_{max}$ and dZ/dt_{max} are identical. Regression equations by Adler et al. [42] and graphic evidence interpolated from Lyssegen et al. [43] show that, at normocardia (70–90 bpm) TTP of $LVdP/dt_{max}$ is 50–60 ms, which is equivalent to the rise time of dZ/dt_{max}. These data suggest that the inotropic forces governing the potential energy generated during isovolumic contraction time (IVCT) are transferred, unabated, converting potential energy to equivalent kinetic energy (as expressed as dv/dt_{max} or equivalently dZ/dt_{max}) during the earliest phase of ejection. Welham et al. [44] have definitively shown that, during halothane-induced myocardial depression $LVdP/dt_{max}$, dv/dt_{max}, and dZ/dt_{max} decrease and recover proportionately with the depth of

anesthesia. With profound myocardial depression, it is easily demonstrated that dZ/dt_{max} peaks synchronously with dv/dt_{max} and appreciably before $Q(t)_{max}$.
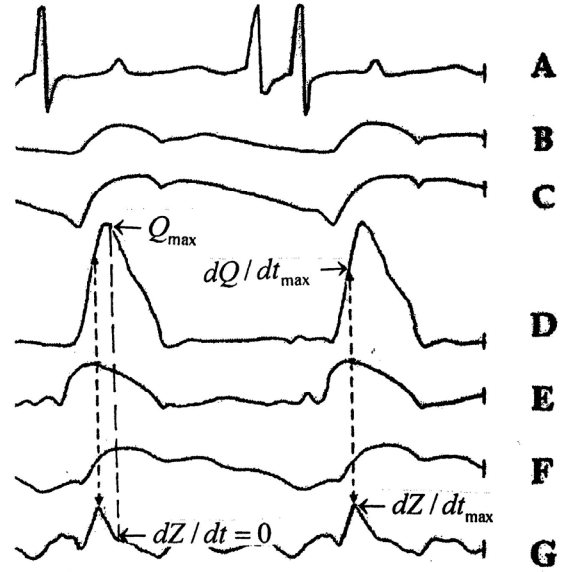

Fig. 6. Relationship between esophageal ECG (A), aortic pressure (B), aortic expansion (C), aortic blood flow (D), pulmonic expansion (E), $\Delta Z(t)$ (F), and dZ/dt (G). Note that dZ/dt_{max} precedes peak aortic blood flow (Q_{max}) during the period of peak flow acceleration in early systole. Modified from reference 13.

Figure 6 shows that dZ/dt_{max} intersects the flow curve during peak acceleration and appreciably before $Q(t)_{max}$. Simultaneously obtained waveforms comparing TTP of peak flow velocity and dZ/dt_{max}, showing the latter temporally preceding the former, can be found elsewhere [30,45,46,47].
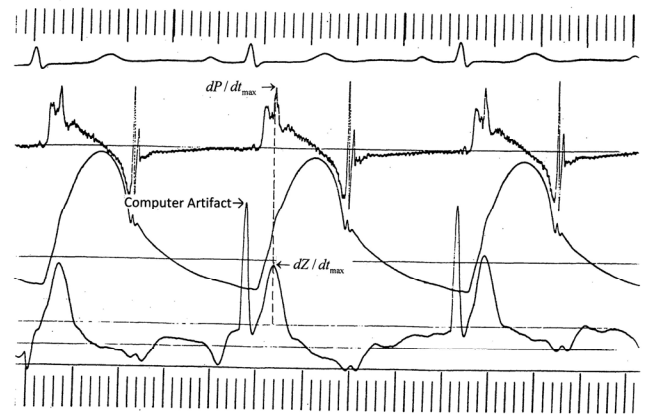

Fig. 7. Ascending aortic dP/dt, ascending aortic pressure P, and dZ/dt from a human. Note that dZ/dt_{max} peaks precisely with ascending aortic dP/dt_{max}. Note computer artifact. Courtesy of Kirk L. Peterson, M.D.; From the cardiac catheterization laboratory at the University of California School of Medicine, San Diego.

Figure 7 shows that dZ/dt_{max} peak synchronously with aortic dP/dt_{max}, where, as extrapolated from equation 9 and its following discussion (*vide supra*) dP/dt_{max} corresponds in time with dF/dt_{max} (major derivative) when dA/dt_{max} (minor derivative) is trivial. This indicates that the peak rate of change of force of ventricular ejection is manifest as dZ/dt_{max} in impedance cardiography. As equations 9 and 11

predict and figure 1 indicates, $Q(t)_{max}$ will occur synchronously with dA/dt_{max}, when aortic dP/dt, dF/dt and $dQ/dt=0$.

Figure 6 indicates that, at $Q(t)_{max}$, $dZ/dt = 0$. These observations infer, if not prove that dZ/dt_{max} occurs in earliest systole, contemporaneously with aortic dP/dt_{max} and peak blood flow acceleration (dv/dt_{max}, dQ/dt_{max}). Further proof that dZ/dt_{max} peaks with and is the electrical analog of dv/dt_{max} is verified experimentally by their corresponding relationship with the "I" wave of the ultra-low frequency acceleration ballistocardiogram (aBCG). Winter et al. [48] showed that the "I" wave of the aBCG corresponds precisely in time with peak aortic blood acceleration dv/dt_{max}, while both Kubicek [49] and Mohapatra and Hill [50] demonstrated that the "I" wave corresponds precisely in time with dZ/dt_{max} (fig 8). Seitz and McIlroy [51] demonstrated that peak blood acceleration and the "I" wave of the HJ interval occur 40–50 ms after opening of the aortic valve, which is consistent with the TTP of dZ/dt_{max}. Consistent with figure 7, showing that dZ/dt_{max} peaks with aortic dP/dt_{max}, Reeves et al. [52] demonstrated that the "I" wave of the aBCG peaks with the second derivative of the carotid contour volume displacement curve (i.e. carotid dP/dt_{max}, pressure acceleration).
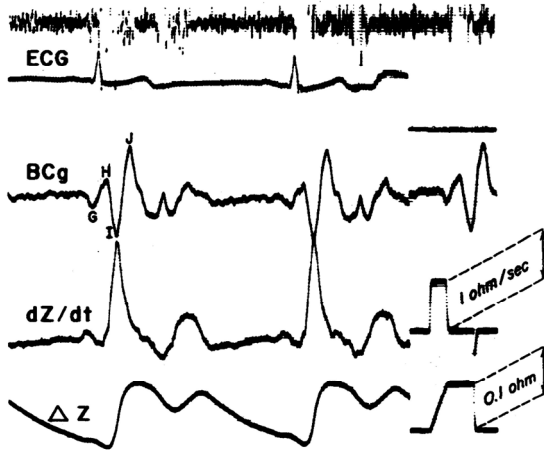

Fig. 8. ECG, ultra-low frequency ballistocardiogram (BCg), dZ/dt, and $\Delta Z(t)$ from a human. Note that the "I" wave of the HJ interval peaks precisely with dZ/dt_{max}. The unlabeled noisy signal above ECG is a phonocardiogram. From reference 49.

Gaw et al. [23] showed that the relative blood conductivity change ($\Delta\sigma/\sigma$ (%), i.e. $[\Delta\rho_b(t)/\rho_b]^{-1}$(%)) parallels the peak acceleration of the red cell reduced average velocity (mean spatial velocity, $<v>/R$ (s^{-1})) with r = 0.99 (fig 4). This implies that the normalized peak rate of change of the blood resistivity variation $d\rho_b(t)/dt_{max}/\rho_{b(stat)}$ is hemodynamically equivalent to the peak rate of change of the red cell reduced average blood acceleration, which is concordant with equation 42. Thus, dZ/dt_{max} appears during the inertial phase of earliest ventricular ejection when little volume change occurs and represents the electrical analog of the most explosive phase of the initial ventricular impulse. Thus, dZ/dt_{max} is bioelectrically equivalent to equation 42 and possesses the units of $\Omega \cdot s^{-2}$.

Square Root Acceleration Step-down Transformation: Ohmic Mean Velocity from Ohmic Mean Acceleration.

As discussed by Gaw [23] and Visser [19], the relative change of blood resistivity (or equivalently blood conductivity) due to aortic blood flow is related, hemodynamically, to an exponential power (n) of the reduced average blood velocity (i.e. mean spatial velocity) $[(<v>/R)^n, (s^{-1})^n]$. It thus follows that $dZ/dt_{max}/Z_0$ (s^{-2}) is the ohmic analog of peak aortic reduced average blood acceleration (PARABA), this being the mean acceleration divided by the aortic valve radius.

$$\text{PARABA} = \frac{d\langle v\rangle/dt_{max}}{R} \quad (s^{-2}) \qquad (44)$$

Through the relationship for mean flow velocity given by Visser [19], PARABA can be reduced to mean blood flow velocity by square root transformation,

$$\overline{\dot{Q}} = \pi r^3 \sqrt{\left(\frac{d\langle v\rangle/dt_{max}}{R}\right)^m} \quad (mL \cdot s^{-1}) \qquad (45)$$

Preliminary evidence suggests that the exponent m is in the range of 1.15–1.25.

To obtain ohmic mean velocity (s^{-1}) from the mean acceleration analog, $dZ/dt_{max}/Z_0$ must also undergo square root transformation.

$$\sqrt{\frac{L^2}{V_b}\frac{d\rho_b(t)}{dt_{max}}\frac{1}{Z_0}} = \sqrt{\frac{dZ/dt_{max}}{Z_0}} \quad (s^{-1}) \qquad (46)$$

It naturally follows that,

$$\sqrt{\left(\frac{d\langle v\rangle/dt_{max}}{R}\right)^m} \equiv \sqrt{\frac{dZ/dt_{max}}{Z_0}} \quad (s^{-1}) \qquad (47)$$

Inasmuch as dZ/dt_{max} is the electrodynamic equivalent of mean aortic blood acceleration, and SV is obtained from a mean velocity calculation, it is suggested that equations 35, 37, and 38 produce a mean acceleration surrogate of SV, which is impossible according to equation 6. Thus,

$$SV = \pi r^2 \int_{t_0}^{t_1} v(t)dt \neq V_{EPT}\frac{dZ/dt_{max}}{Z_0}T_{LVE} \Rightarrow$$

$$SV = C\int_{t_0}^{t_1}\frac{dP(t)}{dt} + \frac{1}{R_s}\int_{t_0}^{t_1}P(t)dt \neq V_{EPT}\frac{dZ(t)/dt_{max}}{Z_0}T_{LVE} \quad (48)$$

Based on the above discussion, this leads to the inevitable conclusion that,

$$SV = \pi r^2 \int_{t_0}^{t_1} v(t)dt = \pi r^2 \cdot \bar{v} \cdot T_{LVE} = V_{EPT} \sqrt{\frac{dZ/dt_{max}}{Z_0}} T_{LVE} \qquad (49)$$

In view of this discussion, the outflow correction factor, dZ/dt_{max} x T_{LVE}, is rendered moot, because dZ/dt_{max} represents axial blood acceleration and not radially-oriented rate of change of volume according to *windkessel* theory [36]. Close correspondence between the Kubicek or Sramek-Bernstein equations with reference method CO is simply due to the fact that peak velocity and mean acceleration are highly correlated (r=0.75) and both peak and mean aortic blood acceleration are highly correlated with SV (r = 0.75) as well as with the systolic velocity integral (stroke distance) (r = 0.75) [53–55]. Thus over a selected range of ohmic acceleration (i.e. dZ/dt_{max}), dZ/dt_{max} × T_{LVE} provides acceleration facsimiles of ohmic mean velocity.

As per equation 46, the relationship between ohmic mean velocity and ohmic mean acceleration is parabolic (ohmic mean acceleration = (ohmic mean velocity)^2 or y = x^2. This relationship predicts that, over wide ranges of dZ/dt_{max}, ohmic mean velocity will be overestimated and underestimated at its upper and lower extremes, respectively.
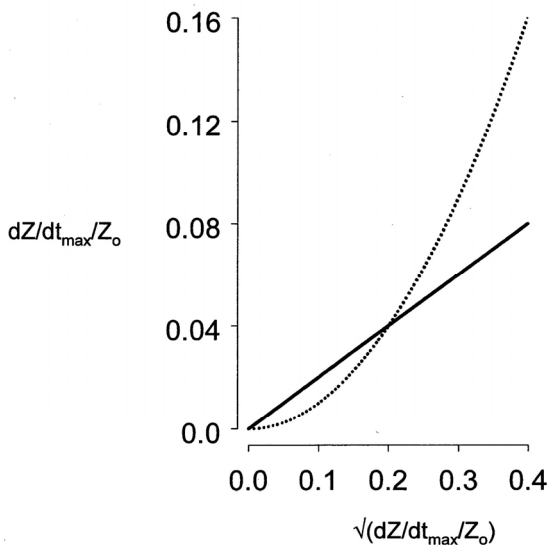

Fig. 9. Square root acceleration step-down transformation. On the y-axis, the ohmic equivalent of peak aortic reduced average blood acceleration (PARABA), which is $dZ/dt_{max}/Z_0$., and the linear extrapolation of the square root transformation, ohmic mean velocity on the x-axis (x = √y and y = x^2). From reference 13.

Indeed, Yamakoshi et al. [1] showed that ICG-derived SV overestimates reference method SV in healthy canines by as much as 70%, and correspondingly underestimates reference SV by as much as 25% when myocardial failure is induced. Similarly, Ehlert and Schmidt [56] could not find a linear relationship between ICG and EMF-derived SV over a wide range of hemodynamic perturbations.

Effect of Hematocrit on dZ/dt_{max} and ICG-Derived SV and CO

As inferred, the static specific resistance of blood, ρ_b, nor the static specific resistance of the thorax, ρ_T, are included in the ohmic acceleration-based SV method. Despite Visser's [19] and Hoetink's [22] *in vitro* experimental findings, showing that the relative blood resistivity change is proportional to hematocrit, Visser et al. [14] also showed that, although the peak magnitude of $\Delta Z_b(t)$ (i.e $\Delta Z_b(t)_{max}$) is hemocrit-dependent, its maximum upslope, dZ/dt_{max}, is not (figure 3 in Visser et al.). In a canine model, Quail et al. [31] showed that normovolemic hemodilution over a hematocrit range of 66%–26%, produced an appropriate increase in SV, which was not different from electromagnetic flow-meter-derived (EMF) SV. Corroboratively, an *in vivo* ICG study by Wallace et al. [57] showed that, over a wide range of hematocrit (20%–35%) and blood conductivity (ρ=80–160Ω·cm) induced by normovolemic hemodilution, ICG CO was in agreement with transit time flow probe CO.

The Volume Conductor (V_{EPT}, V_C)

In contrast to the earlier methods, where the swept volume of the thorax (or portion thereof) is considered the appropriate V_C, the V_{EPT} corresponding to the new method is conceptualized physiologically and by magnitude as the intrathoracic blood volume (ITBV, V_{ITBV}). As opposed to linear-based volume conductors, using thoracic length or a height-based equivalent, ITBV is biophysically assumption-free, inherently unambiguous in physiologic meaning and intuitively understood as the physical embodiment of the blood resistance, R_b. Physiologically, ITBV has been shown to be highly correlated with left ventricular preload, as expressed by left ventricular end-diastolic volume (LVEDV), and thus with absolute values for SV and directional changes thereof [58–61]. Computationally, V_{ITBV} is found through linear allometric equivalents of body mass (kg). Supporting this relationship, studies show that body mass correlates linearly, and much more closely with total blood volume (TBV), SV and CO than patient height [62–66]. By magnitude, the ITBV represents approximately 25% of TBV, or about 17.5 mL·kg^{-1}, which results in V_{ITBV} = 17.5 x W_{kg}, or equivalently $16W_{kg}^{1.02}$ [37,67] By comparison, existing volume conductors associated with the plethysmographic hypothesis are modeled as simple geometric abstractions, which are firmly rooted in basic electrical theory. By virtue of their "best-fit" mathematical construction, they bare little relevance to, and have virtually no biophysical relationship with other commonly accepted physiologic, anatomic, or hemodynamic parameters.

Determinants of the Magnitude of dZ/dt_{max}

Evidence suggesting that dZ/dt_{max} varies inversely with aortic valve CSA, or radius r, as a function of

PARABA, is inferentially demonstrated through the work of Sageman [68]. He clearly showed that an inversely proportional and highly negatively correlated ($r = -0.75$) relationship exists between $dZ/dt_{max}/Z_0$ and body mass in healthy humans. Aortic valve CSA has been shown to correlate highly with body mass (kg) and body surface area (BSA, m^2). But by contrast with $dZ/dt_{max}/Z_0$, Doppler and EMF peak velocities and systolic velocity integrals are totally independent of body mass [69]. Thus, Newtonian-based peak velocities of equal magnitude, measured between age-matched individuals of different body mass and aortic valve CSAs, will produce correspondingly disparate values of $dZ/dt_{max}/Z_0$. It follows that, while there is no direct proportionality between hemodynamically-based and impedance-derived systolic velocity integrals within or between individuals, a linear equivalence exists through their respective mean flow values. Specifically, as a convoluted abstraction of the equation of continuity,

$$Area \times \bar{v} = Volume \times \sqrt{\frac{dZ/dt_{max}}{Z_0}} \quad (mL \cdot s^{-1}) \quad (50)$$

Because of the absolute dependency of $dZ/dt_{max}/Z_0$ upon PARABA, this means that, for any given value of mean acceleration, the magnitude of dZ/dt_{max} is related to and explicitly dependent on aortic root CSA by its dependency on R. Since aortic root CSA is a function of body mass, age, and gender, dZ/dt_{max} will vary accordingly. Thus, the magnitude of dZ/dt_{max} is multi-factorial and not wholly dependent on the respective levels of myocardial contractility and Z_0. As a first order approximation,

$$\frac{dZ(t)}{dt_{max}} = Z_0 \left[\frac{\pi r^3}{V_C} \left(\sqrt{\left(\frac{d\langle v \rangle / dt_{max}}{R} \right)^m} \right) \right]^2 \quad (\Omega \cdot s^{-2}) \quad (51)$$

Index of Transthoracic Aberrant Conduction: Genesis of the Three-Compartment Parallel Conduction Model

One of the major drawbacks of the impedance technique has been its inability to correctly predict SV in the presence of excess EVLW [70–72]. Critchley et al. [73] tested the hypothesis that the poor agreement between invasive reference standards and ICG is due to excess EVLW. Typified by Sepsis, they were able to show that ICG CO underestimated its thermodilution counterpart and that the degree of underestimation was related to the degree of EVLW excess. They also noted that, in general, excess EVLW was associated with values of $Z_0 < 20$–22Ω. In a subsequent experimental model in canines, where pulmonary edema was induced by oleic acid infusion, they found a systematic progressive bias between flow probe and ICG CO [74]. As pulmonary edema progressively worsened, ICG CO progressively underestimated the flow probe estimate. In concert with the progressive divergence of the two methods, Z_0 progressively decreased (fig. 10).

Expanding equation 30, the following is a useful analytical tool for studying the effect of excess EVLW on the various compartments of the transthoracic impedance with the AC field.
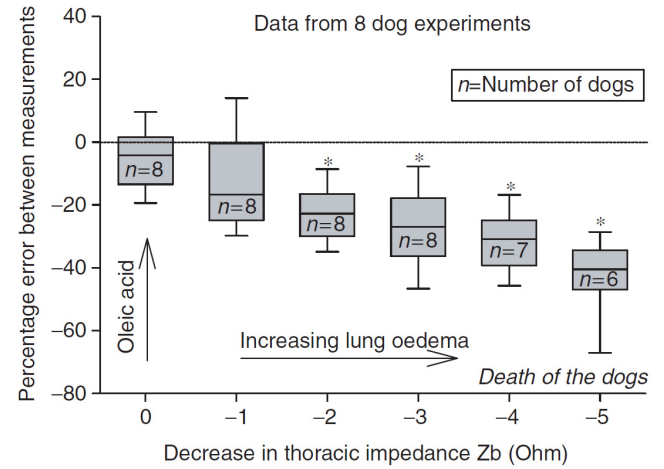

Fig. 10. Box plots showing that, as oleic acid-induced pulmonary edema worsened, as reflected by decreasing Z_0, the systematic underestimation of flow-probe CO by ICG-derived CO increased. From reference 74.

$$I(t) \left[\left(\frac{\rho_t L^2}{V_{t(1)}} \left\| \frac{\rho_b L^2}{V_{b(2)}} \right\| \frac{\rho_e L^2}{V_{e(3)}} \right) \left(\frac{\Delta \rho_b(t) L^2}{V_b} + \frac{\rho_b L^2}{\Delta V_b(t)} \right)_{(4)} \right] = U_0 \| \Delta U_b(t)$$

$$(52)$$

In this model it is assumed that AC ($I(t)$) flows exclusively through the blood resistance Z_b ($100\Omega \cdot cm$–$180\Omega \cdot cm$) (element 2), despite the fact that Z_e (element 3) is of lower specific resistance ($60\Omega \cdot cm$–$70\Omega \cdot cm$). This assumption is probably not accurate, because the blood resistance R_b is considered a cylindrical conductor surrounded by a more highly conductive EVLW impedance Z_e. By the reciprocal rule for parallel impedances, the resultant impedance (i.e. $Z_b \| Z_e$) would be lower than either impedance alone. If Z_e is of variable magnitude and Z_b is held constant, then Z_0 should vary with Z_e. This is precisely what is observed clinically. When Z_e reaches a critical volume ($V_{e(CRIT)}$), Z_e becomes the lowest impedance as relates to the components of Z_0. This causes electrical shunting, and in the extreme case ($Z_0 = 10\Omega$–12Ω), a complete short circuiting of current away from the blood resistance. This results in preferential flow through Z_e at the expense of Z_b, with the result being a decrease in the magnitude of Z_0 and the amplitude of $\Delta Z_b(t)$ [1]. At this critical level of Z_0 (i.e. $Z_{0(CRIT)}$, Z_C), which in humans is $20\Omega \pm 3\Omega$, excess EVLW causes spuriously reduced values of dZ/dt_{max}. Thus, dZ/dt_{max} no longer parallels its hemodynamic equivalent, PARABA, resulting in systematic underestimation of ICG SV/CO. In order to compensate for pathologic conduction through excess EVLW, an index of transthoracic aberrant conduction has been derived (ζ, zeta), which, as its magnitude decreases, creates a larger V_{EPT}.

In patients without excess EVLW, V_{EPT} is equivalent to V_{ITBV}. For all values of $Z_0 < 20\ \Omega$, $0 < \zeta < 1$ and for $Z_0 \geq 20\ \Omega$, $\zeta = 1$. For all values of $Z_0 < 20\ \Omega$, the following pertains:

$$V_{EPT} = \frac{V_{ITBV}}{\zeta^2} \equiv V_{ITBV} + V_{EVLW} \qquad (mL) \qquad (53)$$

where ζ is given as [37],

$$\zeta = \frac{Z_C{}^2 - Z_0 Z_C + K}{2Z_C{}^2 + Z_0{}^2 - 3Z_C Z_0 + K} \quad \text{(Dimensionless)} \quad (54)$$

where Z_C = critical level of base impedance $Z_{0(CRIT)} = 20\Omega$, corresponding to $V_{e(critical)}$. Z_0 = measured transthoracic impedance $\leq Z_C$, and K = a trivial constant $\rightarrow 0$.

Stroke Volume Equation for Impedance Cardiography

$$SV_{ICG} = \frac{V_{ITBV}}{\zeta^2} \sqrt{\frac{dZ(t)/dt_{max}}{Z_0}} T_{LVE} \qquad (mL) \qquad (55)$$

where $V_{ITBV} = 16W_{(kg)}{}^{1.02}$. Equation 55 [37] has been prospectively tested in critical and non-critically-ill patients and been shown to provide SV and CO values comparable to standard reference methods [37,75–78]. As reviewed and compiled by Moshkovitz et al. [7] there are other whole body and transthoracic equations, but they have not been effectively prospectively tested.

Conclusions

From the results of this review, it is strongly suggested that the conceptually-based plethysmographic hypothesis for ICG-derived CO is flawed. The incontrovertible evidence provided herein shows quite conclusively that dZ/dt_{max} is a mean acceleration analog and not that of the peak rate of change of aortic volume. Therefore, to obtain ohmic mean velocity from $dZ/dt_{max}/Z_0$, square root transformation is obligatory. Because dZ/dt_{max} represents axial blood acceleration, the "outflow compensation" for runoff is entirely irrelevant as a theoretical problem to be proved or disproved, as per the work of Faes et al. (36). The fact that dZ/dt_{max} is a mean acceleration analog permits the square wave integration, dZ/dt_{max} x T_{LVE}, as a valid convention similar to equations 6 and 49 for the Doppler/EMF method of SV determination. As for the volume conductors implemented by both the Nyboer/Kubicek and Sramek/Bernstein models, there seems little physiologic justification for either approach. The volume of electrically participating thoracic tissue involved in dynamic conduction is clearly the blood resistance. By magnitude, the blood resistance translates directly into the intrathoracic blood volume. While basing the volume conductor on a fixed volume appears to be concordant with the Sramek/Bernstein model, this can only be true when dynamic conduction through the blood resistance is in parallel with peak aortic reduced average

blood acceleration. This can only occur, when, by volume, the blood resistance is the compartment with the lowest impedance. Thus, when excess extravascular lung water exceeds some critical volume, current is diverted to the compartment of lowest impedance, which is now that of the extravascular lung water. With progressive diversion of AC away from the blood resistance, the magnitude of $\Delta Z_b(t)$ and dZ/dt_{max} diminish and therefore are not reflective of or proportional to the hemodynamic state. Clearly, a more robust mathematical solution for excess extravascular lung water is desirable; that is, if is at all possible.

References

1. Yamakoshi K, Togawa T, Ito H. Evaluation of the theory of cardiac-output computation from transthoracic impedance plethysmogram. Med Biol Eng Comput 1977;15:479–88.

2. Bernstein DP. Pressure pulse contour-derived stroke volume and cardiac output in the morbidly obese patient. Obes Surg 2008;18:1015–21.

3. Quick CM, Berger DS, Noordergraaf A. Apparent arterial compliance. Am J. Physiol (Heart Circ Physiol 43) 1998;274:H1393–1403.

4. Fogliardo R, Di Donfrancesco M, Burattini R. Comparison of linear and nonlinear formulations of the three-element winkdessel model. Am J Physiol (Heart Circ Physiol 40) 1996;271:H2661–68.

5. Chemla D, Hebert J-L, Coirault C, et al. Total arterial compliance estimated by stroke volume-to-aortic pulse pressure ratio in humans. Am J Physiol (Heart Circ Physiol 43)1998;274:H500–05.

6. Olufsen MS, Ottesen JT, Tran HT, et al. Blood pressure and blood flow variation during postural change from sitting to standing: model development and validation. J Appl Physiol 2005;99:1523–37.

7. Moshkovitz Y, Kaluski E, Milo O, et al. Recent developments in cardiac output determination by bio-impedance: comparison with invasive cardiac output and potential cardiovascular applications. Curr Opin Cardiol 2004;19:229–37.

8. Summers RL, Shoemaker WC, Peacock DF, et al. Bench to bedside: electrophysiologic and clinical principles of non-invasive hemodynamic monitoring using impedance cardiography. Acad Emerg Med 2003;10:669–80.

9. Newman DG, Callister R. The non-invasive assessment of stroke volume and cardiac output by impedance cardiography: a review. Aviat Space Environ Med. 1999;70:780–9.

10. Woltjer HH, Bogaard HJ, deVries PM. The technique of impedance cardiography. Eur Heart J 1997;18:1396–403.

11. Kauppinen PK, Hyttinen JA, Malmivuo JA. Senstitivity distributions of impedance cardiography using band and spot electrodes analyzed by a three-dimensional computer model. Ann Biomed Eng 1998;26:694–702.

12. Raaijmakers E, Faes TJ, Scholten RJ, et al. A meta-analysis of three decades of validating thoracic impedance cardiography. Crit Care Med 1999;27:1203–13.

13. Bernstein DP. Impedance cardiography: development of the stroke volume equations and their electrodynamic and biophysical foundations. In: Leondes CT, editor. Bio-

mechanical systems technology: cardiovascular systems. Singapore: World Scientific; 2007. p. 49–87.

14. Visser KR, Lamberts R, Zijlstra WG. Investigation of the origin of the impedance cardiogram by means of exchange transfusion with stroma free haemoglobin solution in the dog. Cardiovasc Res 1990;24:24–32.

15. Visser KR, Lamberts R, Zijlstra WG. Investigation of the parallel conductor model of impedance cardiography by means of exchange transfusion with stroma free haemoglobin solution. Cardiovasc Res 1987;21:637–45.

16. Wang L, Patterson R. Multiple sources of the impedance cardiogram based on 3-D finite difference human thorax models. IEEE Trans Biomed Eng 1995;42:141–8.

17. Geddes LA, Sadler C. The specific resistance of blood at body temperature. Med Biol Eng Comput 1973;11:1973.

18. Sakamoto K, Kanai H. Electrical characteristics of flowing blood. IEEE Trans Biomed Eng 1979;26:686–95.

19. Visser KR. Electrical properties of flowing blood and impedance cardiography. Ann Biomed Eng. 1989;17:463–73.

20. Kosicki J, Chen LH, Hobbie R, et al. Contributions to the impedance cardiogram waveform. Ann Biomed Eng 1986;14:67–80.

21. Ravi Shankar TM, Webster JG, Shao SY. The contribution of vessel volume change and blood resistivity change to the electrical impedance pulse. IEEE Trans Biomed Eng 1985;32:192–98.

22. Hoetink AE, Faes TJ, Visser KR et al. On the flow dependency of the electrical conductivity of blood. IEEE Trans Biomed Eng 2004;51:1251–61.

23. Gaw RL, Cornish BH, Thomas BJ. The electrical impedance of pulsatile blood flowing through rigid tubes: a theoretical investigation. IEEE Trans Biomed Eng 2008;55:721–27.

24. Saito Y, Goto T, Terasaki H, et al. The effects of pulmonary circulation pulsatility on the impedance cardiogram. Arch Int Physiol Biochim 1983;91:339–44.

25. Ito H, Yamakoshi KI, Yamada A. Physiological and fluid-dynamic investigations of the transthoracic impedance plethysmography method for measuring cardiac output. Part II-Analysis of the transthoracic impedance wave by perfusing dogs. Med Biol Eng Comput 1976;14:373–8.

26. Yamakoshi KI, Ito H, Yamada A, et al. Physiological and fluid-dynamic investigations of the transthoracic impedance plethysmography method for measuring cardiac output: Part 1-A fluid-dynamic approach using an expansible tube model. Med Biol Eng Comput 1976;14:365–72.

27. Nyboer J. Electrical impedance plethysmogrphy; a physical and physiologic approach to peripheral vascular study. Circulation 1950;2:811–21.

28. Lamberts R, Visser KR, Zijlstra WG. Impedance Cardiography. Assen, The Netherlands, Van Gorcum; 1984.

29. Kubicek WG, Karnegis JN, Patterson RP et al. Development and evaluation of an impedance cardiac output system. Aerosp Med 1966;37:1208–12.

30. Kubicek WG, Kottke J, Ramos MU, et al. The Minnesota impedance cardiograph-theory and applications. Biomed Eng 1974;9:410–16.

31. Quail AW, Traugott FM, Porges WL, et al. Thoracic resistivity for stroke volume determination in impedance cardiography. J Appl Physiol 1981;50:191–95.

32. Bernstein DP. A new stroke volume equation for thoracic electrical bioimpedance: theory and rationale. Crit Care Med 1986;14:904–09.

33. Feldschuh J, Enson Y. Prediction of the normal blood volume. Relation of blood volume to body habitus. Circulation 1977;56:605–12.

34. Djordjevich L, Sadove MS, Mayoral J, et al. Correlation between arterial blood pressure levels and (dZ/dt)min in impedance plethysmography. IEEE Trans Biomed Eng 1985;32:69–73.

35. Brown CV, Shoemaker WC, Wo CC, et al. Is noninvasive hemodynamic monitoring appropriate for the elderly critically injured patient? J Trauma 2005;58:102–7

36. Faes TJ, Raaijmakers E, Meijer JH, et al. Towards a theoretical understanding of stroke volume estimation with impedance cardiography. Ann NY Acad Sci 1999;873:128–34.

37. Bernstein DP, Lemmens HJ. Stroke volume equation for impedance cardiography. Med Biol Eng Comput 2005;43:443–50.

38. Gardin JM, Burn CS, Childs WJ, et al. Evaluation of blood flow velocity in the ascending aorta and main pulmonary artery of normal subjects by Doppler echocardiography. Am Heart J 1984;107:310–19.

39. Matsuda Y, Yamada S, Kuragane H, et al. Assessment of left ventricular performance in man with impedance cardiography. Jpn Circ J 1978;42:945–54.

40. Lozano DL, Norman G, Knox D, et al. Where to B in dZ/dt. Psychophysiology 2007;44:113–19.

41. Debski TT, Zhang Y, Jennings JR, et al. Stability of cardiac impedance measures: aortic valve opening (B point) detection and scoring. Biol Psychol 1993;36:63–74.

42. Adler D, Nikolic SD, Pajaro O, et al. Time to dP/dtmax reflects both inotropic and chronotropic properties of cardiac contraction. Physiol Meas 1996;17:287–95

43. Lyseggen E, Rabben SI, Skulstad H, et al. Myocardial acceleration during isovolumic contraction: relationship to contractility. Circulation 2005;111:1362–9.

44. Welham KC, Mohapatra SN, Hill DW, et al. The first derivative of the transthoracic electrical impedance as an index of changes in myocardial contractility in the intact anaesthetized dog. Intensive Care Med 1978;4:43–50.

45. Kim DW. Detection of physiologic events by impedance. Yonsei Med J 1989;30:1–11.

46. Rubal BJ, Baker LE, Poder TC. Correlation between maximum dZ/dt and parameters of left ventricular performance. Med Biol Eng Comput 1980;18:541–8.

47. Barbacki M, Gluck A, Sandhage K. Estimation of the correlation between the transcutaneous aortic flow velocity curve and impedance cardiogram in normal children. Cor Vasa 1981;23:291–8.

48. Winter PJ, Deuchar DC, Noble MI, et al. Relationship between the ballistocardiogram and the movement of blood from the left ventricle in the dog. Cardiovasc Res 1967;1:194–200.

49. Kubicek WG. On the source of peak first time derivative (dZ/dt) during impedance cardiography. Ann Biomed Eng 1989;17:459–62.

50. Mohapatra SN, Hill DW. Origin of the impedance cardiogram. In: Mohapatra SN. Non-invasive cardiovascular monitoring by electrical impedance technique. London: Pitman Medical Limited.;1981. P. 41.

51. Seitz WS, McIlroy MB. Interpretation of the HJ interval of the normal ballistocardiogram based on the principle of conservation of momentum and aortic ultrasonic Doppler velocity measurements during left ventricular ejection. Cardiovasc Res 1988;22:571–74.

52. Reeves TJ, Hefner LL, Jones WB, et al. Wide frequency range force ballistocardiogram: its correlation with cardiovascular dynamics. Circulation 1957;16:43–53.

53. Kolettis M, Jenkins BS, Webb-Peploe MM. Assessment of left ventricular function by indices derived from aortic flow velocity. Br Heart J 1976;38:18–31.

54. Sohn S, Kim HS. Doppler aortic flow velocity measurements in healthy children. J Korean Med Sci 2001;16:140–4.

55. Wallmeyer K, Wann LS, Sagar KB, et al. The influence of preload and heart rate on Doppler echocardiographic indexes of left ventricular performance: comparison with invasive indexes in an experimental preparation. Circulation 1986;74:181–6.

56. Ehlert RE, Schmidt HD. An experimental evaluation of impedance cardiographic and electromagnetic measurements of stroke volumes. J Med Eng Technol 1982;6:193–200.

57. Wallace AW, Salahieh A, Lawrence A, et al. Endotracheal cardiac output monitor. Anesthesiology 2000;92:178–89.

58. Rex S, Brose S, Metzelder S, et al. Prediction of fluid responsiveness in patients during cardiac surgery. Br J Anaesth 2004;93:782–8.

59. Della Rocca G, Costa GM, Coccia C, et al. Preload index: pulmonary artery occlusion pressure versus intrathoracic blood volume monitoring during lung transplantation. Anesth Analg 2002;95:835–43.

60. Godje O, Peyerl M, Seebauer T, et al. Central venous pressure, pulmonary capillary wedge pressure and intrathoracic blood volumes a preload indicators in cardiac surgery patients. Eur J Cardiothorac Surg 1998;13:533–9.

61. Kumar A, Anel R, Bunnell E, et al. Pulmonary artery occlusion pressure and central venous pressure fail to predict ventricular filling volume, cardiac performance, or the response to volume infusion in normal subjects. Crit Care Med 2004;32:691–99.

62. Lindstedt L, Schaeffer PJ. Use of allometry in predicting anatomical and physiologic parameters of mammals. Lab Anim 2002;36:1–19.

63. Feldschuh J, Enson Y. Prediction of normal blood volume: relation of blood volume to body habitus. Circulation 1977;56:605–12.

64. Collis T, Devereux RB, Roman MJ, et al. Relations of stroke volume and cardiac output to body composition: the strong heart study.Circulation 2001;103:820–5.

65. West GB, Brown JH, Enquist BJ. A general model for the origin of allometric scaling laws in biology. Science 1997;276:122–6.

66. Holt JP, Rhode A, Kines H. Ventricular volumes and body weight in mammals. Am J Physiol 1968;215:704–15.

67. Hofer CK, Zalunardo P, Klaghofer R, et al. Changes in intrathoracic blood volume associated with pneumoperitoneum and positioning. Acta Anaesthesiol Scand. 2002;46:303–8.

68. Sageman WS. Reliability and precision of a new thoracic electrical bioimpedance monitor in a lower body negative pressure model. Crit Care Med 1999;27:1986–90.

69. Goldman JH, Schiller NB, Lim DC, et al. usefulness of stroke distance by echocardiography as a surrogate marker of cardiac output that is independent of gender and size in a normal population. Am J Cardiol 2001;87:499–502.

70. Young JD, McQuillan P. Comparison of thoracic electrical bioimpedance and thermodilution for the measurement of cardiac index in patients with severe sepsis. Br J Anaesth 1993:70:58–62.

71. Raaijmakers E, Faes TJ, Kunst PW, et al. The influence of extravascular lung water on cardiac output measurements using thoracic impedance cardiograph. Physiol Meas 1998;19:491–9.

72. Genoni M, Pelosi P, Romand JA, et al. Determination of cardiac output during mechanical ventilation by electrical bioimpedance or thermodilution in patients with acute lung injury: effects of positive end-expiratory pressure. Crit Care Med 1998;26:1441–5.

73. Critchley LA, Calcroft RM, Tan PY, et al. The effect of lung injury and excessive lung fluid, on impedance cardiac output measurements, in the critically ill. Intensive Care Med. 2000;26:679–85.

74. Peng ZY, Critchley LA, Fok BS. An investigation to show the effect of lung fluid on impedance cardiac output in the anaesthetized dog. Br J Anaesth 2005;95:458–64.

75. Schmidt C, Theilmeier G, Van Aken H, et al. Comparison of electrical velocimetry and transoesophageal Doppler echocardiography for measuring stroke volume and cardiac output. Br J Anaesth 2005;95:603–10

76. Suttner S, Schollhorn T, Boldt J, et al. Noninvasive assessment of cardiac output using thoracic electrical bioimpedance in hemodynamically stable and unstable patients after cardiac surgery: a comparison with pulmonary artery thermodilution. Intensive Care Med 2006;32:1253–8.

77. Norozi K, Thrane L, Manner J, et al. Electrical velocimetry for measuring cardiac output in children with congenital heart disease. Br J Anaesth 2008;100:88–94.

78. Zoremba N, Bickenbach J, Krauss B, et al. Comparison of electrical velocimetry and thermodilution techniques for the measurement of cardiac output. Acta Anaesthesiol Scand 2007;51:1314–9.